Digital Object Identifier 10.1109/IMFW49589.2021.9642344

2021 IEEE MTT-S International Microwave Filter Workshop (IMFW)

Fully Inline and Symmetric Dual-Mode Dual-Band Bandpass Filters for Millimetre-wave Applications

Chad Bartlett
Michael Höft

Suggested Citation

C. Bartlett and M. Höft, "Fully Inline and Symmetric Dual-Mode Dual-Band Bandpass Filters for Millimetre-wave Applications," *2021 IEEE MTT-S International Microwave Filter Workshop (IMFW)*, 2021, pp. 323-325.

Fully Inline and Symmetric Dual-Mode Dual-Band Bandpass Filters for Millimetre-wave Applications

Chad Bartlett and Michael Höft
Chair of Microwave Engineering, Institute of Electrical Engineering and Information Technology,
Faculty of Engineering, Kiel University,
Kiel, Germany
{chb, mh}@tf.uni-kiel.de

***Abstract*—This work presents the design of inline dual-mode dual-band bandpass filters with flexible center-frequency allocation for application at millimetre-wave frequencies. In this design, resonators are configured for the TE101 and TM120 modes without perturbations or tuning means and allow for the control of two separate fourth-order passbands within the filter while remaining fully inline and symmetric. A presentation on the basic filter design and several examples with different center-frequency locations are presented within the W-band. A prototype with center frequencies at approximately 86.3 GHz and 100 GHz is fabricated and tested. The measurements demonstrate exceptional unloaded Q-factor results for the W-band, ultimately, validating the design approach.**

***Index Terms*—Dual-band bandpass filter (DBBPF), dual-mode, millimetre-wave, TE101, TM120, waveguide filter, W-band**

I. Introduction

As trends for future satellite and wireless communications continue well into the millimetre and sub-millimetre wave regions, many emerging technologies such as silicon micro-machining and additive manufacturing have gained attention in the literature as potential candidates for future large-scale manufacturing. Although these technologies have much potential, high-precision computer numerical control (CNC) milling has also greatly progressed in the recent decade to meet the demands of highly sensitive and micro-fine detailed components. As a few examples in regards to CNC-milled filter design, [1]–[5] have been able to achieve a high level of detail and have demonstrated good measured results throughout the W-band region. Since waveguide technology is still the dominant choice in industry due to its performance capabilities, designs for future millimetre-wave applications will require constant adaptation to meet the stringent constraints imposed by industry such as weight and size. One method of overcoming these constraints is through the use of multi-band systems. These systems can overcome many challenges by utilizing components for both transmission and reception while maintaining a high level of stability and reliability. In regards to millimetre-wave design, only a few cavity-based filters have been demonstrated for dual-band use in the literature; where [6]–[8] have used silicon-wafer and SU-8 micro-machining in the WR-3 band for dual-band Chebyshev responses, and [4], [5] and [9] have used CNC milling to demonstrate dual-band Chebyshev and dual-band quasi-elliptical responses in the WR-10 band. In all but two of these designs ([8], [9]), separated propagation paths are utilized to create the dual-band filter effect, where [8] demonstrates the use of back-to-back SU-8 quadruplets and [9] demonstrates the use of dual-mode cylindrical cavities for fixed center-frequency positions.

Although many high-frequency cavity-based filter designs can be scaled easily to lower frequency bands, the inverse, however, poses inherent fabrication challenges such as infeasible dimensional tolerances, or the use of perturbations and tuning means which become difficult or impractical to implement. In order to overcome these fabrication challenges, we present a novel dual-band filter design with fourth-order Chebyshev responses in each of the passbands by utilizing the TE101 and TM120 modes of rectangular waveguide cavities. The key attributes from this design come in the following form and are therefore demonstrated for W-band operation: flexible center-frequency allocation, single-path propagation, no required perturbations or tuning means for modal excitation, high unloaded Q-factor and remaining fully inline and symmetric. To this end, an experimental prototype of the filter is demonstrated for center-frequency operation at approximately 86.3 GHz and 100 GHz with bandwidths of approximately 2.73 GHz and 2.5 GHz, respectively. Additionally, several instances of the filter profile are simulated for demonstration of the center-frequency allocation.

II. Filter Design

For the design of the filter structure, four rectangular cavities are selected in a manner that support the TE101 and TM120 resonating modes and are positioned in sequential order with inline capacitive irises as the electrical interconnect. In this manner, each of the modes share a common resonator and follow a single propagation path through the filter. A perspective view of the filter's vacuum shell and the electrical topology are depicted in Fig. 1(a) and (b), respectively. Each mode provides a fourth-order Chebyshev response in their respective passband. The 3-dimensional view of the filter that has been presented in Fig. 1(a) is further defined in Fig. 1(c) and Table 1 for three instances of the filter with varying center frequencies; Filter 1 has been selected for fabrication. The

This project has received funding from the European Union's Horizon 2020 research and innovation programme under the Marie Skłodowska-Curie grant agreement 811232-H2020-MSCA-ITN-2018.

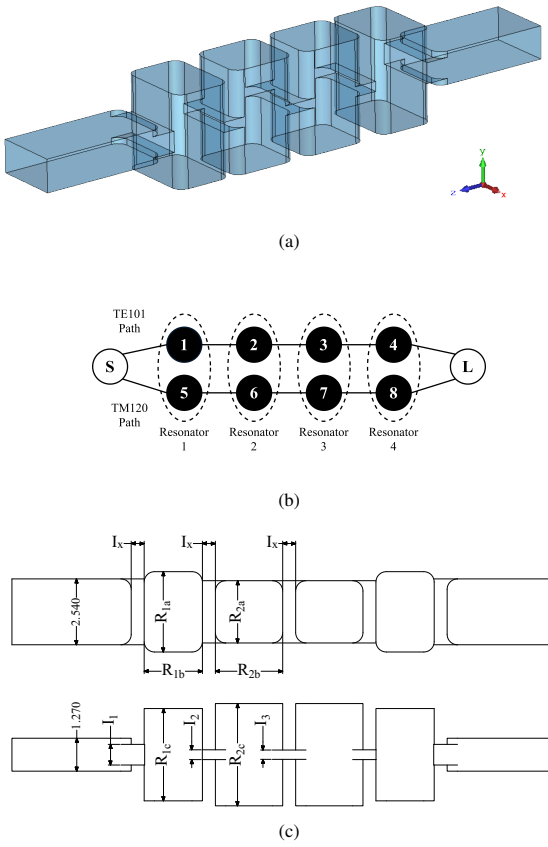

Fig. 1. Filter overview. (a) Perspective view of the dual-mode dual-band filter's vacuum shell, (b) the topology path of the dual-mode dual-band filter; resonating nodes are black and the source/load nodes are white. Solid lines indicate the direct coupling paths and dashed lines indicate the dual-mode resonator sections, and (c) the dual-mode dual-band filter dimensions (mm). See Table 1 for further details.

generalized coupling matrix for Filter 1 can be described from the multi-band synthesis method presented in [10], [11] as (1) at the top of the next page.

The coupling matrix profile and simulations for Filter 1 from (1) and Table 1 are presented in Fig. 2, where the passbands are designated at approximately 86.3 GHz and 100 GHz. Due to the coupling remaining in-phase throughout the filter, the

TABLE I.
Filter Dimensions (in mm)

Dimension	Filter 1 Simulation	Filter 2 Simulation	Filter 3 Simulation
R_{1a}	3.098	2.820	3.784
R_{1b}	2.247	2.372	2.105
R_{1c}	3.560	3.820	3.292
R_{2a}	2.402	2.284	2.266
R_{2b}	2.596	2.764	2.800
R_{2c}	3.944	4.284	3.964
I_1	0.796	0.902	0.768
I_2	0.378	0.500	0.404
I_3	0.360	0.500	0.454
I_x	0.500	0.500	0.500

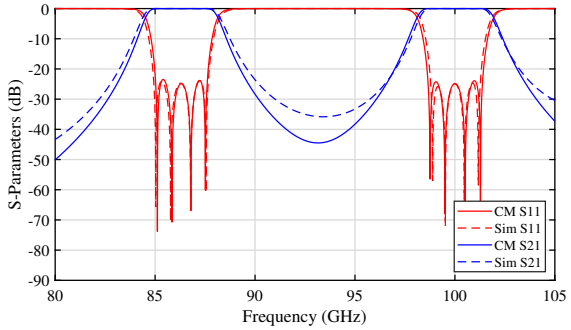

Fig. 2. S-parameters of the coupling matrix profile from (1) and the simulated lossless S-parameters of Filter 1 (see Fig. 1(c) and Table 1 for dimensions).

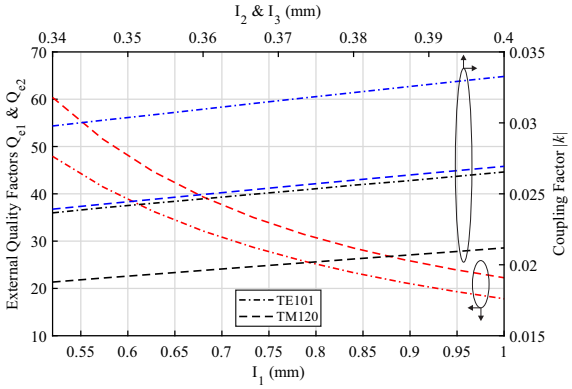

Fig. 3. External quality factor and coupling values while varying the capacitive iris height for Filter 1's defined resonator structures. The dashed-dotted lines indicate the TE101 mode and the dashed lines indicate the TM120 mode, where the red color corresponds to Q_{e1} and Q_{e2}'s dependence on I_1, and the blue and black colors correspond to the coupling factor k's dependence on I_2 and I_3, respectively.

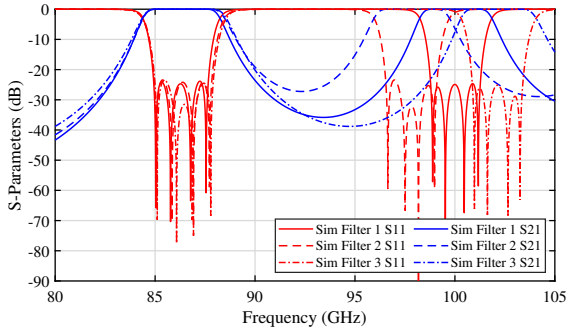

Fig. 4. Demonstration of the passband allocation for three simulated instances of the filter design. The lossless simulated return loss and insertion loss are shown for the filter dimensions given in Table 1 for Filters 1 through 3.

prominence of a transmission zero between the passbands is diminished [10], [11]. Fig. 3 demonstrates the effect on the external quality factor and coupling values when varying the capacitive iris dimensions of Fig. 1(c) for the synchronous and asynchronous resonators that are defined in Table 1 for Filter 1. In Fig. 4, the three instances of this filter with similar bandwidths is presented in order to demonstrate the ability to control the center-frequency locations. Each of the filter's

$$[M] = \begin{bmatrix} 0 & 1.169 & 0 & 0 & 0 & 1.122 & 0 & 0 & 0 & 0 \\ 1.169 & 5.395 & 1.075 & 0 & 0 & 0 & 0 & 0 & 0 & 0 \\ 0 & 1.075 & 5.235 & 0.810 & 0 & 0 & 0 & 0 & 0 & 0 \\ 0 & 0 & 0.810 & 5.235 & 1.075 & 0 & 0 & 0 & 0 & 0 \\ 0 & 0 & 0 & 1.075 & 5.395 & 0 & 0 & 0 & 0 & 1.169 \\ 1.122 & 0 & 0 & 0 & 0 & -5.405 & 0.985 & 0 & 0 & 0 \\ 0 & 0 & 0 & 0 & 0 & 0.985 & -5.245 & 0.740 & 0 & 0 \\ 0 & 0 & 0 & 0 & 0 & 0 & 0.740 & -5.245 & 0.985 & 0 \\ 0 & 0 & 0 & 0 & 0 & 0 & 0 & 0.985 & -5.405 & 1.122 \\ 0 & 0 & 0 & 0 & 1.169 & 0 & 0 & 0 & 1.122 & 0 \end{bmatrix}. \quad (1)$$

(a)

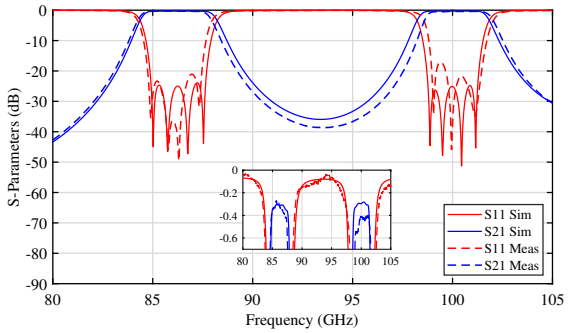

(b)

Fig. 5. Fabrication and Measurements. (a) Image of internal resonators (left), close-up view of internal resonators (center) and the assembled dual-mode dual-band filter (right), and (b) comparison of the lossy simulated (conductivity of brass taken as 1.59e+07 S/m) and measured results.

dimensions are defined in Table 1 with respect to Fig. 1(c). In this demonstration, the lower frequency passbands are held at relatively the same position while the upper center-frequency passbands are swept around the 100 GHz region. The center frequencies of the upper passband for simulations of Filter 2 and Filter 3 are approximately 97.81 GHz and 102.13 GHz, respectively.

III. Fabrication and Results

For the fabrication of Filter 1 as defined in Table 1 and (1), brass has been selected as the cutting material due to its machinability and final surface finish. The filter is split into two separate blocks along the H-plane for high-precision CNC milling with internal radii of 0.4 mm. Fig. 5(a) depicts the milled internal structures for one half of the filter as well as an image of the assembled filter.

Once fabricated and assembled, the filter was tested using a Rohde & Schwarz ZVA67 with W-band up-converters. Fig. 5(b) presents a comparison of the simulated and measured results over 80 GHz to 105 GHz. This direct comparison demonstrates good measured results; the measured return loss is better then 21 dB and 17 dB throughout the lower and upper passbands, respectively, and the measured insertion loss is better than 0.33 dB and 0.42 dB at 86.3 GHz and 100 GHz, respectively. Analyzing the individual passbands, the unloaded quality factors are approximately $Q_{u\_lower} \approx 1860$ and $Q_{u\_upper} \approx 1780$ for the lower and upper passbands, respectively.

IV. Conclusion

A new dual-mode dual-band bandpass filter that utilizes the TE101 and TM120 modes of rectangular resonators has been presented for operation in the W-band. A demonstration of the simulated results for three different filters with similar dimensions exhibits the design flexibility when choosing the operating center frequencies; the basic dimensions are tabulated for each filter. A prototype filter has been fabricated and the measurements demonstrate exceptional response in both of the passbands, therefore, allowing the design to be verified.

References

[1] J. Xu, J.-Q. Ding, Y. Zhao, and J.-X. Ge, "W-band broadband waveguide filter based on H-plane offset coupling," *J. Infrared, Millim., THz Waves*, vol. 40, no. 4, pp. 412–418, 2019.

[2] C. A. Leal-Sevillano, J. R. Montejo-Garai, J. A. Ruiz-Cruz, and J. M. Rebollar, "Low-loss elliptical response filter at 100 GHz," *IEEE Microw. Wireless Compon. Lett.*, vol. 22, no. 9, pp. 459–461, 2012.

[3] C. Bartlett and M. Höft, "W-band TE102-mode filter with doubly loaded E-plane and H-plane irises," *Electron. Lett.*, vol. 57, no. 4, pp. 190–192, 2021.

[4] K. Zhou, J.-Q. Ding, C.-X. Zhou, and W. Wu, "W-band dual-band quasi-elliptical waveguide filter with flexibly allocated frequency and bandwidth ratios," *IEEE Microw. Wireless Compon. Lett.*, vol. 28, no. 3, pp. 206–208, 2018.

[5] J. Chen, S. Zhang, C. Zhang, and Y. Li, "W-band dual-band waveguide band-pass filter using dual-mode cavities," *Electron. Lett.*, vol. 54, no. 25, pp. 1444–1446, 2018.

[6] Y. Huang, X. Li, J. Bao, X. Zhao, Y. Zheng, Y. Du, and Y. Wang, "WR-3 dual-band bandpass filter based on parallel coupling structure," *Microsyst. Technol.*, vol. 23, no. 7, pp. 2553–2559, 2017.

[7] X. Cao, Z. Tang, and J. Bao, "Design of a dual-band waveguide filter based on micromachining fabrication process," *IET, Microw. Antennas Propag.*, vol. 10, no. 4, pp. 459–463, 2016.

[8] X. Shang, M. Ke, Y. Wang, and M. J. Lancaster, "WR-3 band waveguides and filters fabricated using SU8 photoresist micromachining technology," *IEEE Trans. THz Sci. Technol.*, vol. 2, no. 6, pp. 629–637, 2012.

[9] C. Bartlett and M. Höft, "Dual-mode dual-band bandpass filter design utilising cylindrical TM-mode cavities," *Electron. Lett.*, vol. 57, no. 8, pp. 328–330, 2021.

[10] L. Zhu, "High-Q multi-band filters," Ph.D. dissertation, Dept. Elec. and Comp. Eng., University of Waterloo, 2019.

[11] L. Zhu, R. R. Mansour, and M. Yu, "Triple-band cavity bandpass filters," *IEEE Trans. Microw. Theory Tech.*, vol. 66, no. 9, pp. 4057–4069, 2018.